ELSEVIER

Journal of Power Sources 85 (2000) 212–223

JOURNAL OF POWER SOURCES

www.elsevier.com/locate/jpowsour

Determination of reaction resistances for metal-hydride electrodes during anodic polarization

Chunsheng Wang [a], Manuel P. Soriaga [a,*], Supramaniam Srinivasan [b]

[a] *Department of Chemistry, Texas A&M University, College Station, TX 77843, USA*
[b] *Center for Energy and Environmental Studies, Princeton University, Princeton, NJ 08544, USA*

Received 21 May 1999; accepted 14 June 1999

Abstract

The anodic polarization process in metal-hydride electrodes occurs via the following consecutive steps: (i) diffusion of absorbed hydrogen from the bulk to the surface of the electrode, (ii) hydrogen transfer from absorbed state to adsorbed state at the electrode surface, and (iii) electrochemical oxidation of the adsorbed hydrogen on the electrode surface. A theoretical treatment is presented to account for the dependencies on these three consecutive steps, of the reaction resistances, anodic limiting current, cathodic limiting current, and exchange current. The theoretical analysis predicts that the total resistances measured from linear micropolarization is the sum of the charge-transfer, hydrogen-transfer, and hydrogen-diffusion resistances, which is in contradiction with the generally accepted idea that the resistance measured from linear micropolarization is only the charge-transfer resistance. For a metal-hydride electrode with a flat pressure plateau at a low state of discharge (SOD), the resistance measured from linear micropolarization is approximately equal to the sum of three resistances measured from AC impedance, namely, charge-transfer, hydrogen-transfer and hydrogen-diffusion resistances; however, when the SOD is high, the resistance measured from linear micropolarization is higher than total resistances measured from AC impedance.

Keywords: Metal-hydride electrodes; Anodic polarization; Hydrogen

1. Introduction

Nickel/metal hydride (Ni/MH) batteries have been developed and commercialized because of their high energy density, high rate capability, tolerance to overcharge and overdischarge, freedom from poisonous heavy metals, and the absence of consumption of electrolyte during charge–discharge cycles [1a,1b]. The performance of a metal-hydride electrode is determined by the diffusion of absorbed hydrogen from the bulk to the electrode surface, the rate of transfer hydrogen from the absorbed state to the adsorbed state, and the kinetics of electrochemical oxidation of adsorbed hydrogen at the electrode surface [2].

Extensive work has been carried out on the measurement of kinetic parameters of metal-hydride electrodes [3–10]. The exchange current of metal-hydride electrodes can be determined by linear micropolarization ($\eta < 10$ mV) [3,4,6], Tafel polarization [4] and electrochemical impedance spectroscopy (EIS) [4,8]. Witham et al. [4] and Ratnakumar et al. [10] found that exchange currents estimated from linear micropolarization for $LaNi_{5-x}Sn_x$, and $LaNi_{5-x}Ge_x$ ($0 \leq x \leq 0.5$) alloys were in agreement with those from EIS, but were quite different from values obtained from Tafel polarization methods. From electrochemical investigations of bare and Pd-coated $LaNi_{4.25}Al_{0.75}$ electrode in alkaline solution, Zheng et al. [8] believed that the resistances determined from linear micropolarization are the sum of the electrochemical reaction and ohmic resistances, and the total resistance agrees with the sum of three resistances obtained from AC impedance measurements. In a previous paper, we showed that the three resistances in the Nyquist plot represent the charge-transfer reaction, hydrogen-transfer between absorbed and adsorbed states, and hydrogen diffusion in the bulk of alloy, respectively [9]. Hence, the resistance for

* Corresponding author. Tel.: +1-409-845-1846; fax: +1-409-815-3523; E-mail: soriaga@chemvx.tamu.edu

0378-7753/00/$ - see front matter
PII: S0378-7753(99)00336-5

hydrogen transfer at the surface and the resistance for hydrogen diffusion in the alloy may be included in the resistances determined from linear micropolarization curves. The diversity of results from previous impedance measurements may be caused by a neglect of the effect of hydrogen transfer between the absorbed and adsorbed states on the resistance in linear micropolarization and Tafel polarization techniques.

In this paper, we describe results from our investigation of the kinetics of the anodic polarization on a metal-hydride electrode with a flat pressure plateau. Apart from the charge-transfer and hydrogen-diffusion steps, the present treatment considers hydrogen transfer through the interface, a process neglected in previous studies.

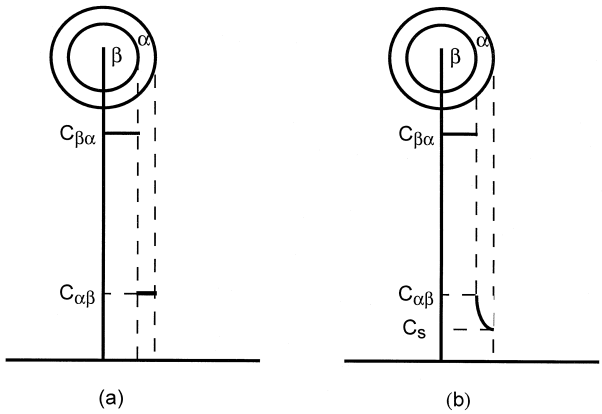

Fig. 2. The hydrogen concentration distribution in a metal-hydride particle: (a) initial state, (b) under anodic polarization.

2. Basic assumptions

The pressure plateau of a hydrogen storage alloy is flat (Fig. 1) and the fully charged hydride electrode with hydrogen concentration $C_{\beta\alpha}$ is initially considered to be uniformly discharged to a state of discharge (SOD). The hydrogen concentration C, expressed in moles of hydrogen atoms stored in the volume unit of the host, is $C_{\beta\alpha}$ in the β phase, and $C_{\alpha\beta}$ in the α phase. The molar quotient of hydrogen concentration in the bulk can be expressed as $X = C/N_m$, where N_m is the total molar number available for hydrogen per unite volume of host metal. The hydrogen distribution before and in anodic polarization are shown in Fig. 2.

The anodic polarization process involves a charge-transfer step followed by the hydrogen transition from the absorbed site in the near-surface to the adsorbed site on the electrode surface, and then the diffusion of absorbed hydrogen from the bulk to the near surface. When the hydrogen concentration of the metal (α) phase at the interface between the α and β phases, X is lower than the hydrogen concentration $X_{\alpha\beta}$, which is the hydrogen concentration of the α phase equilibrating with that of the hydride (β) phase, the β → α phase transition occurs.

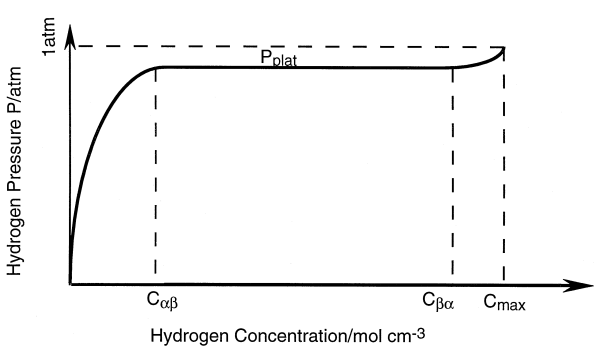

Fig. 1. Typical curve of pressure vs. hydrogen content for a metal-hydride electrode.

$$MH_{ads} + OH^- \underset{k_{-1}}{\overset{k_1}{\Leftrightarrow}} M + H_2O + e^- \quad (1)$$

$$MH_{abs(surface)} \underset{k_{-2}}{\overset{k_2}{\Leftrightarrow}} MH_{ads} \quad (2)$$

$$MH_{abs(bulk)} \overset{\text{diffusion}}{\rightarrow} MH_{abs(surface)} \quad (3)$$

$$MH(\beta) \overset{\text{phase transition}}{\rightarrow} MH(\alpha) \quad (4)$$

During EIS, linear polarization and Tafel polarization measurement, the SOD should not be changed, which means that the phase transformation does not occur. Therefore, steps (1) to (3) are assumed to be responsible for the overpotential associated with the anodic polarization of a metal-hydride electrode.

2.1. Diffusion of hydrogen in the bulk of metal-hydride electrode with spherical symmetry

During anodic polarization, a steady state is assumed to be established; it is therefore reasonable to consider that the hydrogen diffusion is in a steady state and the SOD is not changed during anodic polarization. From Fick's first law and the continuity of H flow in the α phase, the diffusion of hydrogen in the bulk of the metal-hydride electrode, reaction (3), can be expressed as follows [11]:

$$4FD_\alpha N_m \pi r^2 \frac{dX}{dr} = 4FD_\alpha N_m \pi r_0^2 \left.\frac{dX}{dr}\right|_{r=r_o} = 4\pi r_o^2 I_a \quad (5)$$

where F is the Faraday's constant, r_o is the average radius of alloy particles, I_α is the anodic current density, and D_α is the diffusion coefficient of hydrogen in the α phase which is taken as a constant.

Integrating Eq. (5) with the boundary conditions, $r = r_o$, $X = X_s$, and $r = r_\beta$, $X = X_\beta$ gives:

$$X_s = X_{\alpha\beta} - \frac{I_a r_o}{FD_\alpha N_m}\left(\frac{r_o}{r_\beta} - 1\right) \quad (6)$$

where r_β is the radius of the unreacted hydride and X_s is the hydrogen concentration in the near-surface of the electrode. If $\mathrm{SOD} = Q_d/Q_{max}$, then r_o/r_β can be expressed as [11]:

$$\frac{r_o}{r_\beta} = (1 - \mathrm{SOD})^{-1/3} \quad (7)$$

Therefore, Eq. (6) can be rewritten as:

$$X_s = X_{\alpha\beta} - \frac{I_a r_o}{FD_\alpha N_m}\left[(1 - \mathrm{SOD})^{-1/3} - 1\right] \quad (8)$$

The anodic hydrogen diffusion (from bulk to near-surface) limiting current I_{Lbs}, at which the absorbed-hydrogen surface concentration goes to zero, can be obtained by setting in $X_s = 0$ in Eq. (8):

$$I_{Lbs} = \frac{FD_\alpha N_m X_{\alpha\beta}}{r_o\left[(1 - \mathrm{SOD})^{-1/3} - 1\right]} \quad (9)$$

Substitution of Eq. (9) into Eq. (8), one obtains:

$$X_s = X_{\alpha\beta}\left(1 - \frac{I_a}{I_{Lbs}}\right) \quad (10)$$

2.2. Transfer of hydrogen from the absorbed state in the near-surface to adsorbed state on the electrode surface

By assuming first-order kinetics for the absorption reaction, the hydrogen transfer [reaction (2)] can be expressed as [2]:

$$I_a = Fk_2 X_s(1 - \theta) - Fk_{-2}\theta(1 - X_s) \quad (11)$$

where k_2 and k_{-2} are, respectively, the forward and backward rate constants for the hydrogen-transfer reaction, and θ is the coverage of adsorbed hydrogen on the surface. From Eq. (11), one can obtain the dependence of the surface coverage θ on X_s [2]:

$$\theta = \frac{k_2 X_s - \frac{I_a}{F}}{(k_2 - k_{-2})X_s + k_{-2}} \quad (12)$$

At the equilibrium potential, $I_a = 0$, $\eta_a = 0$, $\theta = \theta_o$ and $X = X_{\alpha\beta}$. The equilibrium condition gives [2]:

$$\theta_o = \frac{k_2 X_{\alpha\beta}}{(k_2 - k_{-2})X_{\alpha\beta} + k_{-2}} \quad (13)$$

where θ_o is the initial coverage of adsorbed hydrogen on the surface.

Using I_{La} to denote the anodic limiting current at which the hydrogen coverage goes to zero (i.e., limiting hydrogen-diffusion and hydrogen-transition currents), and substituting X_s from Eq. (10) into Eq. (12), one gets, at $\theta = 0$:

$$\frac{1}{I_{La}} = \frac{1}{Fk_2 X_{\alpha\beta}} + \frac{1}{I_{Lbs}} = \frac{1}{I_{Lbd}} + \frac{1}{I_{Lbs}} \quad (14)$$

where $I_{Lbd}(= Fk_2 X_{\alpha\beta})$ is the limiting current imposed by the hydrogen transfer from the absorbed to adsorbed state.

By substitution of Eq. (14) into Eq. (10), X_s can be rewritten as:

$$X_s = X_{\alpha\beta}\left[1 - \left(\frac{1}{I_{La}} - \frac{1}{I_{Lbd}}\right)I_a\right] \quad (15)$$

When $I_a = 0$, the $X_s = X_{\alpha\beta}$, which mean that the hydrogen concentration of equilibrated α phase (with β phase) is same when the hydrogen pressure plateau is flat as shown in Fig. 1.

Combination of Eqs. (12), (13) and (15), and introduction of a new parameter [2] $K_t(= ((k_2 - k_{-2})X_{\alpha\beta})/((k_2 - k_{-2})X_{\alpha\beta} + k_{-2}))$, which is the interfacial hydrogen-transfer coefficient, one gets:

$$\theta = \frac{\theta_o\left(1 - \frac{I_a}{I_{La}}\right)}{1 - K_t\left(\frac{1}{I_{La}} - \frac{1}{I_{Lbd}}\right)I_a} = \frac{\theta_o\left(1 - \frac{I_a}{I_{La}}\right)}{1 - K_t\frac{I_a}{I_{Lbs}}} \quad (16)$$

where K_t is a parameter which characterizes the relative difficulty of hydrogen transfer from the absorbed to the adsorbed state. If $K_t > 0$, then $k_2 > k_{-2}$, which means that the transfer of hydrogen from the absorbed state occurs more easily than the transfer from a desorbed to absorbed state [2]. The reverse is true if $K_t < 0$.

When Eq. (9) is substituted into Eq. (14), the anodic limiting current I_{La} is obtained:

$$I_{La} = \frac{Fk_2 N_m D_\alpha X_{\alpha\beta}}{k_2 r_o\left[(1 - \mathrm{SOD})^{-1/3} - 1\right] + N_m D_\alpha} \quad (17)$$

From Eq. (17), it can be seen that I_{La} increases with increasing k_2, D_α, N_m, $X_{\alpha\beta}$, but decreases with increasing SOD and r_o.

Although Eq. (16) is deduced from a metal-hydride electrode with a flat pressure plateau and spherical symmetry, it can also be obtained in a more general case (Appendix A). In other words, Eq. (16) is valid for all metal-hydride electrodes.

2.3. Electrochemical oxidation of hydrogen on the electrode surface

The anodic current density for the charge-transfer reaction (Eq. (1)) can be written as [7]:

$$I_a = I_o\left\{\frac{\theta}{\theta_o}\exp\left(\frac{\beta F}{RT}\eta\right) - \frac{1 - \theta}{1 - \theta_o}\exp\left[-\frac{(1 - \beta)F}{RT}\eta\right]\right\} \quad (18)$$

while the exchange current I_o can be expressed as [9]:

$$I_o = Fk_1 a_{OH^-}\theta_o \exp\left(\frac{\beta F}{RT}\varphi_o\right)$$

$$= Fk_{-1} a_{H_2O}(1-\theta_o)\exp\left[-\frac{(1-\beta)F}{RT}\varphi_o\right] \quad (19)$$

where φ_o is the initial potential of the metal-hydride electrode, $\eta(=\varphi-\varphi_o)$ the overpotential, a_{H_2O} and a_{OH^-} the activities of H_2O and OH^-, respectively, k_1 and k_{-1} the forward and reverse rate constants of the charge-transfer reaction, respectively, β the symmetry factor, R the gas constant, and T is the absolute temperature.

2.4. The anodic polarization of metal-hydride electrode

2.4.1. Reaction resistance in AC impedance spectroscopy

In a previous paper [9], a mathematical model was developed for the EIS of a metal-hydride electrode. The equivalent circuit for metal-hydride electrode is shown in Fig. 3. In this figure, R_s, R_{ct}, and R_{ht} are, respectively, the solution, charge-transfer and hydrogen-transfer resistances; C_{dl} and C_{ht} are the double-layer and absorption capacitances, respectively; Z_d is the impedance of hydrogen diffusion in the alloy. For a metal-hydride electrode with a flat pressure (potential) plateau, Z_d can be simplified as a Warburg impedance $[Z_w = \frac{\sigma}{\sqrt{2\omega D_\alpha}}(1-j)]$ in series with a capacitance $[C_1(=r_o(1-X_{\alpha\beta})X_{\alpha\beta})(N_m F^2/RT)]$ in the high-frequency range; at low frequencies, Z_d can be taken as a resistance (R_d) in parallel with a resistance (R)–capacitance (C_d) series (Fig. 4).

Simulations based on the present model show that there are usually three arcs in the Nyquist plot; these represent charge-transfer, hydrogen-transfer, and hydrogen-diffusion steps. The relative frequency range of these three steps in the Nyquist plot depends on the difference of their respective time constants. The arc of the step with a small time constant will appear in the high-frequency range, whereas the arc at low frequency corresponds to the step with the large time constant.

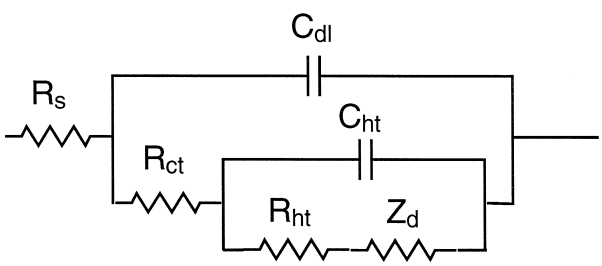

Fig. 3. Equivalent circuit for metal-hydride electrodes.

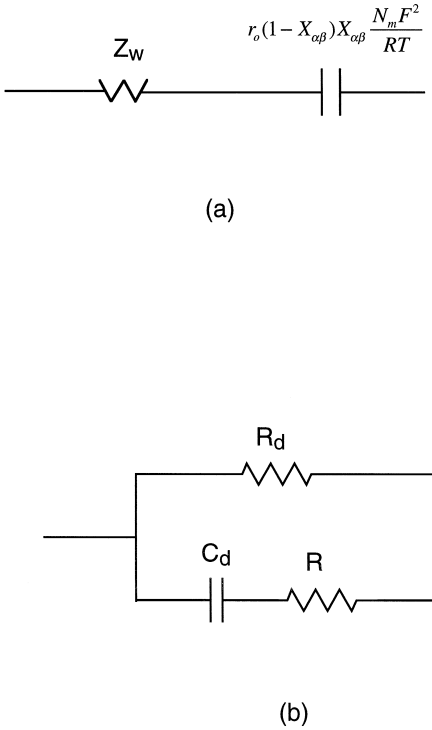

Fig. 4. Equivalent circuit for finite spherical hydrogen diffusion Z_d: (a) in the high-frequency range, (b) in the low-frequency range. $Z_w = \frac{\sigma}{\sqrt{2\omega D_\alpha}}(1-j)$, $C_d = \frac{r_o[1-(1-\mathrm{SOD})^{1/3}]}{3\sigma}$, $R_d = \frac{i\sigma r_o[1-(1-\mathrm{SOD})^{1/3}]}{D_\alpha(1-\mathrm{SOD})^{1/3}}$, $R = \frac{r_o[1-(1-\mathrm{SOD})^{1/3}]\sigma}{5D_\alpha}$.

The parameters for the hydride electrode have been expressed as follows [9]:

$$R_{ct} = \frac{RT}{FI_o} \quad (20)$$

$$R_{ht} = \frac{RT}{F^2 k_{-2}}\left(1+\frac{1}{K_1 A}\right)(1+K_1 K_2 A) \quad (21)$$

$$R_d = \frac{\sigma r_o\left[(1-\mathrm{SOD})^{-1/3}-1\right]}{D_\alpha} \quad (22)$$

$$C_{ht} = \frac{F^2\Gamma}{RT}\left[\sqrt{K_1 A}+\frac{1}{\sqrt{K_1 A}}\right]^{-2} \quad (23)$$

$$C_d = \frac{r_o\left[1-(1-\mathrm{SOD})^{1/3}\right]}{3\sigma} \quad (24)$$

$$Z_d = \frac{\sigma}{\sqrt{j\omega D}\Big/\tanh\left[r_o\left(1-(1-\mathrm{SOD})^{1/3}\right)\sqrt{\frac{j\omega}{D}}\right]-\frac{D}{r_o}} \quad (25)$$

where

$$\sigma = \left(\sqrt{K_1 K_2 A} + \sqrt{\frac{1}{K_1 K_2 A}}\right)^2 \frac{RT}{N_m F^2} \tag{26}$$

$$K_1 = \frac{k_1}{k_{-1}},\ K_2 = \frac{k_2}{k_{-2}}, \tag{27}$$

$$A = \frac{a_{OH^-}}{a_{H_2O}} \exp\left(\frac{F}{RT}\varphi_o\right) \tag{28}$$

$$I_o = \frac{F k_1 a_{OH} \exp\left(\frac{\beta F}{RT}\varphi\right)}{K_1 A + 1} \tag{29}$$

Combination of Eqs. (19) and (28) gives:

$$A = \frac{(1-\theta_o)k_{-1}}{\theta_o k_1} \tag{30}$$

where R_d and C_d are the resistance and capacitor for hydrogen diffusion in the bulk of alloy.

Simulation results indicate that: (i) R_d, not $(R_d + R)$, is the resistance for the equivalent circuit of Z_d in the low-frequency range (Fig. 4b), and (ii) R_d is approximately equal to the resistance calculated from the hydrogen-diffusion impedance Z_d at a low SOD. However, when the SOD is high, R_d is a little larger than the resistance calculated from Z_d in Fig. 3 (vide infra).

The limiting current of a step reflects its reaction rate; hence, the dependence of the parameters on the limiting current can be deduced. Similar to the definitions of the *anodic* hydrogen-transfer limiting current ($I_{Lbd} = Fk_2 X_{\alpha\beta}$), the $Fk_{-2}(1 - X_{\alpha\beta})$ were considered as *cathodic* hydrogen-transfer limiting current (hydrogen transfer from the adsorbed to absorbed state) in Ref. [2] (Eq. (31)). Comparing the *anodic* hydrogen-diffusion limiting current (Eq. (9)), we can consider $(FD_\alpha N_m(1 - X_{\alpha\beta}))/(r_o[(1 - \mathrm{SOD})^{-1/3} - 1])$ as a *cathodic* hydrogen-diffusion limiting current although it is only approximately equal to the real cathodic hydrogen-diffusion limiting current measured from Tafel polarization.

$$Fk_{-2}\left(1 - X_{\alpha\beta}\right) = I_{Ldb} \tag{31}$$

$$\frac{FD_\alpha N_m\left(1 - X_{\alpha\beta}\right)}{r_o\left[(1 - \mathrm{SOD})^{-1/3} - 1\right]} = I_{Lsb} \tag{32}$$

Combination of Eqs. (13), (21)–(32) yields:

$$R_{ht} = \frac{RT}{F}\left(\frac{1}{I_{Lbd}} + \frac{1}{I_{Ldb}}\right) \tag{33}$$

$$R_d = \frac{RT}{F}\left(\frac{1}{I_{Lbs}} + \frac{1}{I_{Lsb}}\right) \tag{34}$$

$$C_{ht} = \frac{F^2 \Gamma}{RT}\left[\sqrt{\frac{I_{Ldb}}{I_{Lbd}}} + \sqrt{\frac{I_{Lbd}}{I_{Ldb}}}\right]^{-2} \tag{35}$$

$$C_d = \frac{F r_o^2\left[1 - (1 - \mathrm{SOD})^{1/3}\right]^2}{3RTD_\alpha\left(\frac{1}{I_{Lbs}} + \frac{1}{I_{Lsb}}\right)(1 - \mathrm{SOD})^{1/3}} \tag{36}$$

$$Z_d = \frac{RT\left(\frac{1}{I_{Lbs}} + \frac{1}{I_{Lsb}}\right)}{F r_o\left[(1-\mathrm{SOD})^{-1/3} - 1\right]\left[\sqrt{j\omega D}\right.} \times \coth\left[r_o(1-(1-\mathrm{SOD})^{1/3})\right]\left.\sqrt{\frac{j\omega}{D_\alpha}} - \frac{D_\alpha}{r_o}\right] \tag{37}$$

$$I_o = \frac{F\sqrt{k_1 k_{-1} a_{H_2O} a_{OH}}}{\sqrt{\frac{I_{Lbd}}{I_{Ldb}}} + \sqrt{\frac{I_{Ldb}}{I_{Lbd}}}} \tag{38}$$

The total resistance measured from AC impedance is:

$$R_{ta} = R_{ct} + R_{ht} + R_d = \frac{RT}{F}\left(\frac{1}{I_o} + \frac{1}{I_{Lbd}} + \frac{1}{I_{Ldb}} + \frac{1}{I_{Lbs}} + \frac{1}{I_{Lsb}}\right) \tag{39}$$

The time constants of three steps can be expressed as follows:Charge-transfer reaction:

$$\tau_e = \frac{RTC_{dl}}{FI_o} \tag{40}$$

Hydrogen-transfer reaction:

$$\tau_a = R_{ht} \times C_{ht} = \frac{F\Gamma}{I_{Lbd} + I_{Ldb}} \tag{41}$$

Hydrogen diffusion:

$$\tau_d = \frac{r_o F N_m\left[1 - (1 - \mathrm{SOD})^{1/3}\right]}{3(I_{Lsb} + I_{Lbs})} \tag{42}$$

It is more convenient to employ dimensionless parameters $\tau_a/\tau_e(= K_{ae})$ and $\tau_d/\tau_e(= K_{de})$ to assess whether the three arcs overlap. When Eqs. (40)–(42) are combined, the following relationships are obtained:

$$K_{ae} = \frac{F^2 I_o \Gamma}{RTC_{dl}(I_{Lbd} + I_{Ldb})} \tag{43}$$

$$K_{de} = \frac{r_o F^2 N_m I_o\left[1 - (1 - \mathrm{SOD})^{1/3}\right]}{3RTC_{dl}(I_{Lsb} + I_{Lbs})} \tag{44}$$

Eqs. (43) and (44) can be used to estimate the relative frequency range of the three steps at a low SOD. The simulation obtained using Eqs. (40) and (42) indicates that the first arc that appears in the higher frequency range is a

charge-transfer reaction, the second arc at intermediate frequencies range represents the hydrogen-transfer reaction, and the third arc at low frequencies corresponds to the diffusion of absorbed hydrogen in the alloy. For example, a $TiMn_{1.5}H_x$ electrode with a double-layer capacitance $C_{dl} = 2 \times 10^{-5}$ F/cm^2, size of a particle $r_o = 10^{-3}$ cm, concentration of absorbed hydrogen $N_m = 0.02$ mol/cm^3, maximum coverage of adsorbed hydrogen $\Gamma_H = 7.5 \times 10^{-10}$ mol/cm^2, Faraday's constant $F = 96{,}487$ C/mol, and a SOD of 10%, has $K_{ae} = (141.34 I_o)/(I_{Lbd} + I_{Ldb})$ and $K_{de} = (4.4 \times 10^4 I_o)/(I_{Lsb} + I_{Lbs})$; this means that a hydrogen-transfer and hydrogen-diffusion limiting current larger than 141.34 and 4.4×10^4 times the exchange current, respectively, are needed for hydrogen transfer and hydrogen diffusion steps appearing in higher frequency range than that for the charge-transfer step. If the values of the hydrogen-transfer and hydrogen-diffusion limiting currents are similar to the anodic or cathodic limiting current, and the anodic limiting current is 4.1–6.2 times larger than the exchange current [5], the frequency range of the three steps appear in decreasing order: *charge transfer > hydrogen transfer > hydrogen diffusion*. If the difference between time constants among the three steps are large, and the difference between resistances are small, the three arcs are well-resolved from one another. But if the SOD is high, or the hydrogen diffusion coefficient is low, the hydrogen-diffusion arc moves toward the lower frequency range; in addition, the radius of the almost circular low-frequency segment increases rapidly such that the arcs of charge-transfer and hydrogen-transfer reactions may overlap with the hydrogen-diffusion arc due to the larger resistance of hydrogen diffusion [9].

2.4.2. Reaction resistances in anodic Tafel polarization

During the anodic polarization process, a steady state is characterized by (i) an equality of the rates for the three consecutive steps, and (ii) a constant in SOD. During anodic Tafel polarization, when $I_o \ll I_{La}$, and $\eta \gg RT/F$, Eq. (18) can be simplified in the following form [2]:

$$\eta = \frac{RT}{\beta F}\ln\frac{I_a}{I_o} + \frac{RT}{\beta F}\ln\frac{\theta_o}{\theta} \tag{45}$$

If $I_o > I_{La}$, then $I_a < I_o$, which will yield a negative electrochemical polarization in Eq. (45). Hence, when $I_o > I_{La}$, Eq. (45) cannot be employed to calculate the polarization and exchange current.

If $I_o \ll I_{La}$, substitution of Eqs. (13) and (16) into Eq. (45) yields:

$$\eta = \frac{RT}{\beta F}\ln\frac{I_a}{I_o} + \frac{RT}{\beta F}\ln\left(\frac{I_{La}}{I_{La} - I_a}\right) + \frac{RT}{\beta F}\ln\left[1 - K_t\left(\frac{1}{I_{La}} - \frac{1}{I_{Lbd}}\right)I_a\right] \tag{46}$$

It can be seen from this equation that the Tafel polarization includes electrochemical polarization, hydrogen-diffusion polarization, and a third polarization associated with a hydrogen-transfer and hydrogen-diffusion reaction. During anodic Tafel polarization, the anodic current increases as the overpotential is increased but, when strongly polarized, a limiting current I_{La} can be observed with its value measurable from Tafel polarization curves.

2.4.3. Reaction resistances in linear micropolarization

For small polarization ($\eta < 10$ mV), the anodic current density for the charge-transfer reaction (Eq. (18)) can be linearized. The reaction resistances R_{lm} can be obtained from a complete Taylor expansion of Eq. (18) (Appendix B):

$$R_{lm} = \frac{\eta}{I_a} = \frac{RT}{F}\left[\frac{1}{I_o} + \frac{\theta_o - \theta}{I_a\theta_o(1-\theta_o)}\right] \tag{47}$$

Substitution of Eqs. (13), (16), (31) and (32) into Eq. (47) gives:

$$R_{lm} = \frac{RT}{F}\left(\frac{1}{I_o} + \frac{\dfrac{1}{I_{Lbd}} + \dfrac{1}{I_{Ldb}} + \dfrac{1}{I_{Lbs}} + \dfrac{1}{I_{Lsb}}}{1 - K_t\dfrac{I_a}{I_{Lbs}}}\right) \tag{48}$$

In a linear micropolarization process, I_a is much lower than I_{Lbs}, and $K_t(I_a/I_{Lbs})$ can be neglected. Eq. (48) can thus be simplified as:

$$R_{lm} = \frac{RT}{F}\left(\frac{1}{I_o} + \frac{1}{I_{Lbd}} + \frac{1}{I_{Ldb}} + \frac{1}{I_{Lbs}} + \frac{1}{I_{Lsb}}\right) \tag{49}$$

Upon comparison with Eq. (39), it can be seen that the resistances measured from linear micropolarization are the same as the sum of the charge-transfer, hydrogen-transfer and hydrogen-diffusion resistances measured from AC impedance techniques. That is,

$$R_{lm} = R_{ta} = R_{ct} + R_{ht} + R_d \tag{50}$$

It can be readily seen from Eq. (50) that the resistance measured from linear micropolarization is the sum of three resistances *in series*: charge-transfer resistance R_{ct}, hydrogen-transfer resistance R_{ht}, and hydrogen-diffusion resistance R_{hd}. This theoretical result is in contradiction with the generally accepted idea that the resistance determined from linear micropolarization arises solely from a charge-transfer reaction. When I_o is much greater than the limiting currents, $R_{ct} \ll R_{ht} + R_{hd}$ and the overpotential, even near E_{eq} is mass-transfer overpotential induced by hydrogen diffusion and hydrogen transfer. Only when I_o is much smaller than the limiting currents, will $R_{ct} \gg R_{ht} + R_{hd}$, and the overpotential near E_{eq} is due to charge-transfer activation.

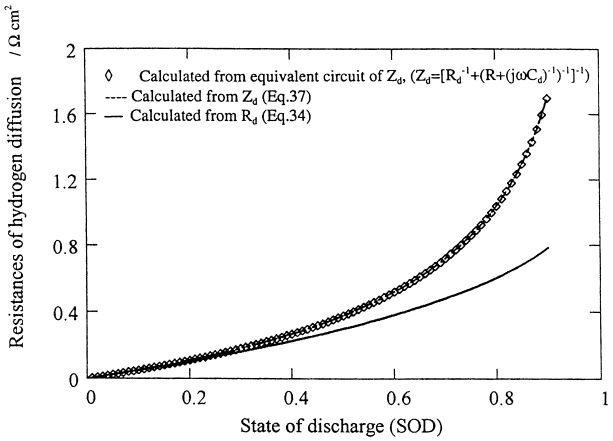

(a)

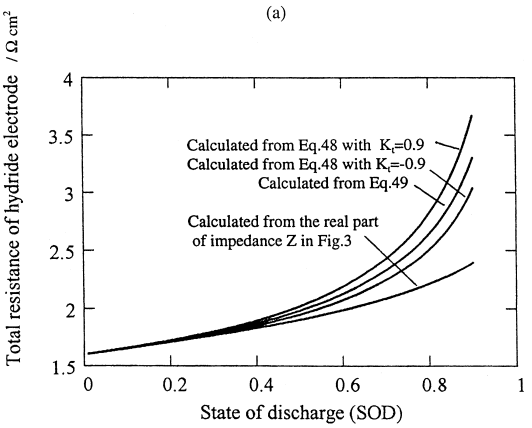

(b)

Fig. 5. The simulated resistances of hydride electrodes at different states of discharge with the parameters in Table 1 and $X_{\alpha\beta} = 0.1$, $I_{lbd} = 0.154$ A/cm^2 s, $I_{ldb} = 0.695$ A/cm^2 s. (a) The hydrogen-diffusion resistances are calculated from the hydrogen-diffusion impedance Z_d (Eqs. (9), (32) and (37)), the equivalent circuit of hydrogen-diffusion impedance, Z_d (parameters in Fig. 4b) and R_d (Eqs. (9), (32) and (34)). The resistance calculated from Z_d is obtained from the real part of Z_d at a low frequency, 0.0005 Hz. (b) The total resistances calculated, respectively, from linear micropolarization at different K_t values [I_a in Eq. (48) was approximated as $0.01/(R_{ct} + R_{ht} + R_d)$] and from the real part of AC impedance spectrum at a low frequency, 0.0005 Hz.

2.5. The relationship of the parameters measured from linear micropolarization, Tafel polarization and AC impedance

Similar to Eq. (14), the cathodic limiting current can be expressed as

$$\frac{1}{I_{Lc}} = \frac{1}{I_{Lsb}} + \frac{1}{I_{Ldb}} \tag{51}$$

I_{Lc} is the cathodic limiting current if the $\alpha \rightarrow \beta$ phase transition does not occur during cathodic polarization. Substitution of Eqs. (14) and (51) into Eq. (50) and rearrangement gives the following equation for R_{lm}:

$$R_{lm} = \frac{RT}{F}\left(\frac{1}{I_o} + \frac{1}{I_{La}} + \frac{1}{I_{Lc}}\right) \tag{52}$$

When combined with Eqs. (20), (50) and (52) yields:

$$\frac{RT}{F}\left(\frac{1}{I_{La}} + \frac{1}{I_{Lc}}\right) = R_{ht} + R_d \tag{53}$$

Eqs. (50), (52) and (53) reveal the relationships between the parameters determined from linear micropolarization, Tafel polarization and AC impedance; i.e., the dependencies of the total resistances measured from linear micropolarization and AC impedance on the parameters measured from Tafel polarization (exchange current I_o, anodic limiting current I_{La} and cathodic limiting current I_{Lc}).

It is worth mentioning that I_{Lc} in the present model is an apparent cathodic limiting current. Its value will be approximately equal to the real cathodic limiting current measured from Tafel polarization if the $\alpha \rightarrow \beta$ phase transformation in cathodic Tafel polarization does not occur and the potential at limiting current is smaller than -0.932 V vs. Hg/HgO, i.e., no hydrogen recombinations occur.

3. Discussion

Although Eq. (50) is deduced from a metal-hydride electrode with flat pressure plateau, it is also applicable to all types of metal-hydride electrodes regardless of the morphology of its pressure plateau; this is because Eq. (50) is derived from Eqs. (13) and (16), both of which can also be deduced from a more general case (Appendix A). Hence, the resistance of metal-hydride electrodes measured from linear micropolarization curves is the total resistance that includes contributions from charge-transfer, hydrogen-transfer and hydrogen-diffusion reactions. However, most treatments of linear micropolarization assume that the resistance measured is only a charge-transfer resistance [3,4,7,10]; the contributions from hydrogen transfer and hydrogen diffusion are simply neglected. As a matter of fact, numerous experiments show that (i) the discharge process for metal-hydride electrodes is controlled by hydrogen diffusion within the bulk [12–14], and (ii) the

Table 1
Parameters used in the simulations

Parameters	Values	Unit	References
a_{H_2O}	0.68		[9]
a_{OH}	1.38×10^{18}		Calculated from Ref. [15]
C_{dl}	2×10^{-5}	F/cm^2	$TiMn_{1.5}$ alloy
D	10^{-8}	cm^2/s	[9]
F	96487	A s/mol	[9]
k_1	5.38×10^{-16}	cm/s	Calculated from Ref. [15]
k_{-1}	4.8×10^{-16}	cm/s	Calculated from Ref. [15]
k_2	1.6×10^{-5}	mol/cm^2 s	[9]
k_{-2}	0.8×10^{-5}	mol/cm^2 s	[9]
N_m	0.2	mol/cm^3	fitted
Γ	7.5×10^{-9}	mol/cm^2	fitted
r_o	10^{-3}	cm^{-3}	[9]

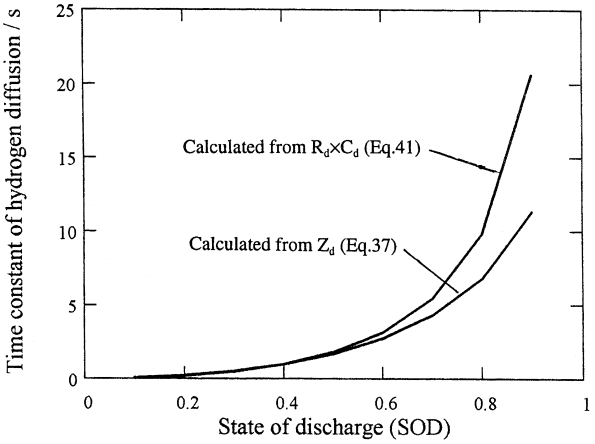

Fig. 6. The time constant of hydrogen diffusion calculated from $R_d \times C_d$ (Eq. (41)) and directly from Z_d, respectively, with the same parameters as in Fig. 5.

anodic overpotential is highly dependent on the surface properties introduced by various surface pretreatments [2]. Such experiments demonstrate the importance of a theoretical treatment that includes not only charge-transfer resistance but also hydrogen-transfer and hydrogen-diffusion resistances during anodic polarization. Zheng et al. [8] recently found that, for $LaNi_{4.25}Al_{0.75}$, the resistance measured from linear micropolarization is approximately equal to the sum of three resistances measured from AC impedance; this is in agreement with predictions based on the present model. However, it was speculated that the other two resistances were (i) the resistance between the current collector and the electrode pellet, and (ii) the alloy particle-to-particle contact resistance. It is our contention that the two arcs in the high-frequency range of the Nyquist plot are due to the charge-transfer and hydrogen-transfer reactions, with the arc at the low-frequency region to be due to hydrogen-diffusion resistance [9]. From the present model, it can be argued that the resistance measured from linear micropolarization is approximately equal to the sum of three (charge-transfer, hydrogen-transfer and hydrogen-diffusion) resistances measured from AC impedance. The approximation arises from (i) the assumption of R_d as the resistance of hydrogen-diffusion impedance Z_d, and (ii) the neglect of the term in Eq. (48) for linear micropolarization.

Fig. 5a shows the hydrogen-diffusion resistances at different states of discharge calculated from hydrogen-diffusion impedance Z_d, the equivalent circuit of Z_d at low-frequency range, and R_d, along with the parameters in Table 1 and: $X_{\alpha\beta} = 0.1$, $I_{Lbd} = 0.154$ A/cm^2 s, and $I_{Ldb} = 0.695$ A/cm^2 s. The resistance calculated from Z_d is obtained from the real part of impedance at a low frequency $\omega = 0.0005$. It can be seen in Fig. 5a that R_d is equal to the resistance of the equivalent circuit of Z_d, but both are larger than the resistance calculated from the hydrogen-diffusion impedance Z_d with increasing SOD. The reason is that the expansion of $\coth[r_o(1-(1-\mathrm{SOD})^{1/3})\sqrt{\frac{j\omega}{D}}]$ of Z_d at the point of $r_o(1-(1-\mathrm{SOD})^{1/3})\sqrt{\frac{j\omega}{D}} = 0$ at low frequencies, only the first three terms in the expansion are selected [9]. When the SOD is low, $r_o(1-(1-\mathrm{SOD})^{1/3})\sqrt{\frac{j\omega}{D}}$ is close to zero, and the relative error is small. However, when the SOD is high, $r_o(1-(1-\mathrm{SOD})^{1/3})\sqrt{\frac{j\omega}{D}}$ is non-zero even in the low-frequency range; this means that the use of only the first three expansion terms leads to inaccuracies. Since the fourth expansion term will be positive, the admittance of hydrogen diffusion is smaller than actual value, while the impedance of hydrogen diffusion would be higher than real value. Hence, the resistance R_d calculated from only the first three expansion terms is larger than the actual value when the SOD is high (Fig. 5a). Neglecting the $K_t I_a / I_{Lbs}$ term likewise causes the resistance determined from linear micropolarization to be approximately equal to $R_{ct} + R_{ht} + R_d$ (Eq. (50)), but the difference in the resistances calculated from Eqs. (48) and (49) is smaller than the difference between R_{lm} and resistance calculated form Z_d (Fig. 5b). Therefore, the resistance determined from linear micropolarization would be higher than the sum of three resistances measured from AC impedance if the SOD is high. Based on the same argument, the hydrogen-diffusion time constant calculated as $R_d \times C_d$ would also be higher than the time constant measured from Z_d as shown in Fig. 6.

The present theoretical analysis has uncovered a relationship between resistance, exchange current, anodic limiting current, and cathodic limiting current (Eqs. (20) and

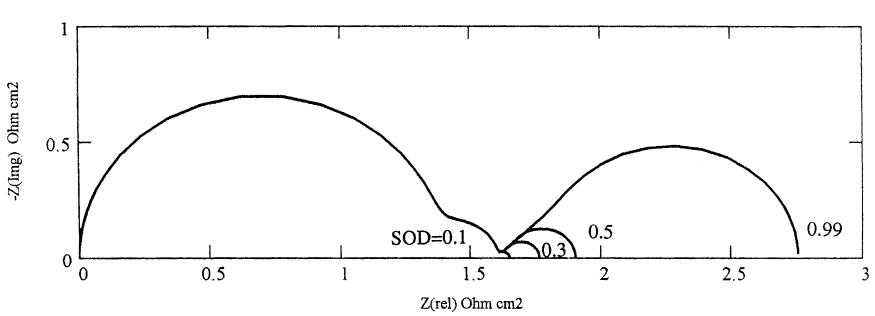

Fig. 7. Simulated Nyquist plot for the hydride electrode with flat pressure plateau at different states of discharge. The simulations are based upon the model in Fig. 3 with the parameters given in Tables 1 and 2.

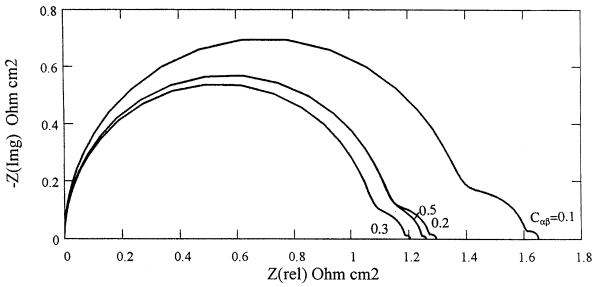

Fig. 8. Simulated Nyquist plot for the hydride electrode with flat pressure plateau at different hydrogen concentrations. The simulations are based upon the model in Fig. 3 with the parameters given in Tables 1 and 2.

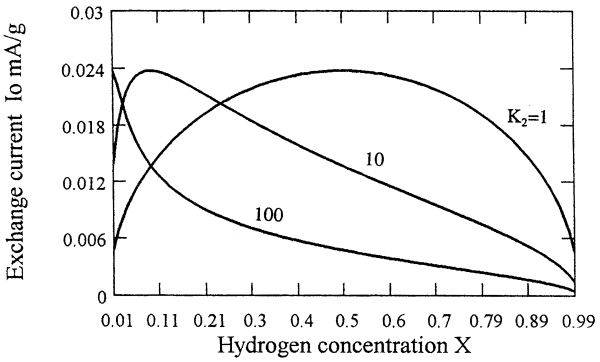

Fig. 9. Exchange currents of hydride electrodes at different K_2 values calculated from Eq. (38) with the parameters of $k_1 = 5.38\times10^{-16}$ cm/s, $k_{-1} = 4.8\times10^{-16}$, $a_{H_2O} = 0.68$ mol/cm^3, $a_{OH^-} = 1.38\times10^{18}$ mol/cm^3, $k_{-2} = 0.8\times10^{-5}$ mol/cm^2 s, $k_{-2} = 0.8\times10^{-5}$ mol/cm^2 s, $X_\alpha = 0.1$.

(53)) as well as a dependence of the anodic and cathodic limiting currents on the SOD and the hydrogen concentration $X_{\alpha\beta}$ (Eq. (17) and the combinations of Eqs. (31), (32) and (51)). The influence of the anodic and cathodic limiting currents on the Nyquist plot can be observed by simulation of the Nyquist plot at different SOD and $X_{\alpha\beta}$ as shown in Figs. 7 and 8, respectively. The parameters used in the present simulation are shown in Table 1, with the exchange current and limiting current values at different SOD and $X_{\alpha\beta}$ given in Table 2. It can be seen in Fig. 7 and Table 2 that the diameter of the low-frequency arc (R_d) increases with decreasing anodic and cathodic limiting currents; the SOD affects the arc only in the low-frequency region. Since, in fact, the pressure plateau of practical hydride electrode is not very flat, $X_{\alpha\beta}$ will decrease with increasing SOD. Fig. 8 shows the influence of $X_{\alpha\beta}$ on the AC impedance. From Fig. 8 and Table 2, one can see that the hydrogen-transfer and hydrogen-diffusion resistances decreases with increasing $X_{\alpha\beta}$, but the exchange current first increases and later decreases as $X_{\alpha\beta}$ is increased; this suggests the existence of an optimum $X_{\alpha\beta}$ value for the exchange current. Differentiation of Eq. (38) with respect to $X_{\alpha\beta}$ allows one to determine the optimum $X_{\alpha\beta}$ value to yield a maximum exchange current:

$$X_{\alpha\beta p} = \frac{1}{K_2 + 1} \tag{54}$$

Fig. 9 shows the relationship between exchange current and K_2, the equilibrium constant for the hydrogen-transfer reaction. From this figure and Eq. (54), it can be ascertained that the optimum hydrogen concentration $X_{\alpha\beta}$ decreases with increasing K_2. When the latter is large, $X_{\alpha\beta}$ is small, and the decrease in exchange current with an increase in $X_{\alpha\beta}$ can easily be observed [8]. In actuality, the value of K_2 is not very high; hence, the exchange current usually increases with $X_{\alpha\beta}$ [15].

Table 2
Resistances, limiting current, and exchange current at different SOD and $X_{\alpha\beta}$

Resistances (Ω cm^2)			Current (A/cm^2)			SOD	$X_{\alpha\beta}$
R_t	R_{ht}	R_d	I_o	I_{La}	I_{Lc}		
1.397	0.203	0.053	0.018	0.12	0.608	0.1	0.1
1.397	0.203	0.165	0.018	0.077	0.462	0.3	0.1
1.397	0.203	0.304	0.018	0.05	0.341	0.5	0.1
1.397	0.203	1.157	0.018	5.123×10^{-3}	0.045	0.99	0.1
1.143	0.124	0.03	0.022	0.24	0.54	0.1	0.2
1.081	0.103	0.023	0.024	0.36	0.473	0.1	0.3
1.143	0.009	0.019	0.022	0.6	0.338	0.1	0.5

Further, use of Tafel polarization curves to measure the exchange current must be done with caution since the Tafel Eq. (46) is valid only when $I_o \ll I_a \leq I_{La}$. Even in such a case, the influence of the hydrogen-transfer reaction on the polarization must be considered in the determination of exchange current. Usually, the exchange current is determined by the following equation obtainable from Eq. (46).

$$\eta = \frac{RT}{\beta F}\ln\frac{I_{La}}{I_o} + \frac{RT}{\beta F}\ln\left(\frac{I_a}{I_{La} - I_a}\right) + \frac{RT}{\beta F}\ln\left[1 - K_t\left(\frac{1}{I_{La}} - \frac{1}{I_{Lbd}}\right)I_a\right] \tag{55}$$

According to Eq. (55), a plot of η-vs.-ln($I_a/(I_{La} - I_a)$) should produce a straight line with slope and intercept, respectively, being $RT/\beta F$ and $(RT/\beta F)\ln(I_{La}/I_a)$ at $\eta \gg (RT/F)$ if $K_t = 0$. In other words, the exchange current I_o can be calculated from I_{La} and $RT/\beta F$ data. However, when K_t is in positive [16] (i.e., hydrogen is transferred more easily from the absorbed to the adsorbed state than in the reverse direction), the η-vs.-ln($I_a/(I_{La} - I_a)$) plot shows a linear relationship between η and ln($I_a/(I_{La} - I_a)$) only in the middle range of polarization; negative deviations from linearity appear at the low-overpotential domain, while positive deviations from linearity emerge at the large-overpotential polarization region (Fig. 10a). In this case, the exchange current density measured from Tafel polarization is lower than actual value. When

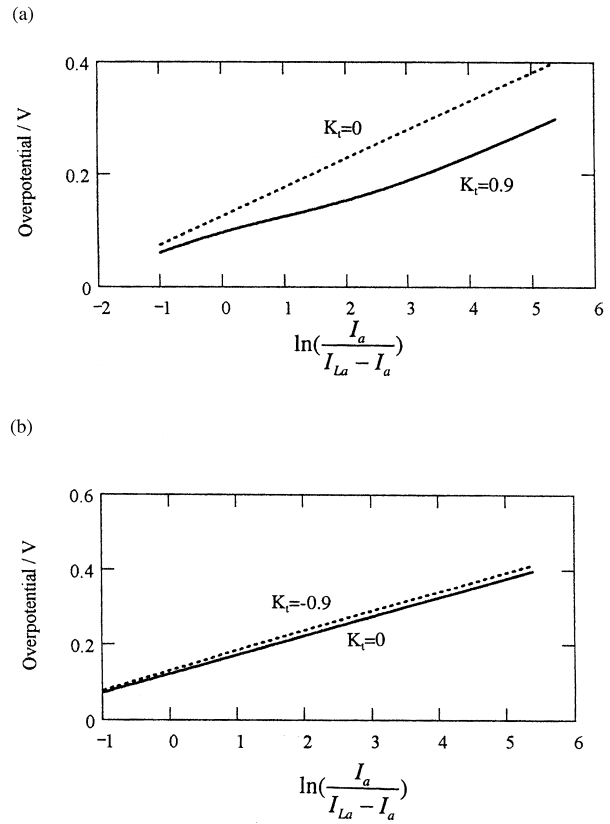

Fig. 10. Overpotential as a function of $\ln(I_a/(I_{La}-I_a))$ for the hydride electrode at different K_t values calculated from Eq. (55) with the parameters: (a) $K_t = 0.9$, $I_{La} = 0.27$, $(1/I_{La})-(1/I_{Lbd}) = 1/0.26$; (b) $K_t = -0.9$, $I_{La} = 0.113$, $(1/I_{La})-(1/I_{Lbd}) = 1/0.26$.

$K_t < 0$, the η-vs.-$\ln(I_a/(I_{La}-I_a))$ curves show a linear relationship between η and $\ln(I_a/(I_{La}-I_a))$ throughout the entire polarization range (Fig. 10b). Under these conditions, the exchange current is a little higher than the actual value.

4. Conclusions

Based on a three-step anodic polarization process (H diffusion from the bulk to the surface, H transfer from absorbed to adsorbed state, and electrochemical oxidation of adsorbed H), a theoretical relationship between (i) the resistances in anodic linear micropolarization, (ii) the exchange currents and anodic and cathodic limiting currents in Tafel polarization, and (iii) the resistance in AC impedance measurements has been obtained. Application of the theory shows that the resistance measured from linear micropolarization is the sum of three resistances: (i) charge-transfer, (ii) hydrogen-transfer, and (iii) hydrogen-diffusion resistances. When the charge-transfer reaction is the rate-determining step, the exchange current can be measured approximately from linear micropolarization or Tafel polarization after correction for the hydrogen-diffusion and hydrogen-transfer effects. If the hydrogen-diffusion limiting current is smaller than the exchange current, the resistance is not controlled by the charge-transfer reaction, and the exchange current cannot be measured directly from linear micropolarization. In this case, the exchange current cannot also be determined from Tafel polarization curves but it can be measured by AC impedance. For metal-hydride electrodes with a flat pressure plateau and low SOD, the resistance measured from linear micropolarization is approximately equal to the sum of the charge-transfer, hydrogen-transfer and hydrogen-diffusion resistances, all three measurable from AC impedance spectroscopy. If the SOD is high, the resistance measured from linear micropolarization is larger than the sum of three resistances measured from AC impedance.

5. List of symbols

a_{H_2O}, a_{OH^-}	activity of H_2O and OH^- in solution, respectively (mol/cm^3)
$C_{\alpha\beta}$, $C_{\beta\alpha}$	hydrogen concentration of α phase equilibrating with β phase and hydrogen concentration of β phase equilibrating with α phase, respectively (mol/cm^3)
C_{dl}, C_d, C_{ht}	double-layer capacitance, capacitance associated with hydrogen diffusion, and hydrogen transfer capacitance, respectively (F/cm^2)
D_α	diffusion coefficient of hydrogen in the α phase of metal-hydride particles (cm^2/s)
F	Faraday's constant (96 487 C/mol)
I_a, I_o	anodic current and exchange current, respectively (A/cm^2)
I_{La}, I_{Lc}	anodic limiting current and cathodic limiting current, respectively (A/cm^2)
I_{Lbs}, I_{Lsb}	limiting current of hydrogen diffusion from the bulk to the surface of particle and limiting current of hydrogen diffusion from the surface to the bulk of particles, respectively (A/cm^2)
I_{Lbd}, I_{Ldb}	limiting current of hydrogen transfer from absorbed state to adsorbed state, and limiting current of hydrogen transfer from adsorbed state to absorbed state, respectively (A/cm^2)
j	$\sqrt{-1}$

k_1, k_{-1}	forward and backward rate constants of charge-transfer reaction, respectively (cm/s)
k_2, k_{-2}	forward and backward rate constants for hydrogen-transfer reaction, respectively (mol/cm^2 s)
$K_1(=k_1/k_{-1})$, $K_2(=k_2/k_{-2})$	equilibrium constant of charge-transfer reaction and hydrogen transfer process, respectively
K_{ae}, K_{de}	ratio of time constant of hydrogen-transfer reaction to time constant of charge-transfer reaction, and ratio of time constant of hydrogen diffusion to time constant of charge-transfer reaction, respectively
N_m	available concentration of absorbed hydrogen (mol/cm^3)
R_s, R_{ct}, R_{ht}, R_d	solution resistance, charge-transfer reaction resistance, hydrogen-transfer reaction resistance, and hydrogen-diffusion resistance, respectively (Ω cm^2)
r_o, r_β	radius of alloy particles and radius of untransformed hydride-core phase (cm)
SOD	state of discharge
$X(=C/N_m)$, $X_s, X_{\alpha\beta}(=C_{\alpha\beta}/N_m)$	relative concentration of hydrogen in α phase, relative concentration of hydrogen at the surface of the electrode, and relative concentration of hydrogen in α phase equilibrating with β phase, respectively
Greek	
β	symmetry factor in the oxidation direction
θ, θ_o, Γ	coverage degree of adsorbed hydrogen, equilibrium (initial) coverage of adsorbed hydrogen, maximum coverage degree of adsorbed hydrogen on the electrode surface (mol/cm^2)
φ, φ_o	potential and equilibrium (initial) potential of hydride electrode, respectively (V)
$\eta(=\varphi-\varphi_o)$	overpotential of hydride electrode (V)
ω	angular frequency of ac single
τ_a, τ_e, τ_d	time constant of hydrogen-transfer reaction, time constant of charge-transfer reaction, and time constant of hydrogen diffusion, respectively (s)
σ	impedance coefficient of hydrogen diffusion

Acknowledgements

The work was performed under the auspices of the US Department of Energy, Division of Chemical Sciences, Office of Basic Energy Science (Contract No. DE-AC02-76CH00016, BNL and DE-FG03-93ER1481). The assistance of M.R. Marrero (Texas A&M University), D. Barsellini (INIFTA, La Plata, Argentina) and Dr. H.G. Pan (Zhejiang University of China) are gratefully acknowledged. Support for the collaborative work with INIFTA was made possible by the National Science Foundation (INT-9813852).

Appendix A

In the absence of migration, the rate of mass transfer is proportional to the concentration gradient at the electrode surface, which can be approximated by $N_m((X_o - X_s)/\delta)$, where δ is the thickness of the hypothetical diffusion layer at the electrode surface, and X_o is the initial concentration of hydrogen in the bulk. The hydrogen diffusion rate can be express as

$$I_a = FD\frac{X_o - X_s}{\delta} \tag{A-1}$$

When anodic current increases to limiting current I_{La}, at which the hydrogen coverage goes to zero, X_s would decrease to X_s^*. The relationship between I_{La} and X_s^* can be obtained from Eq. (12) at $\theta = 0$

$$I_{La} = Fk_2 X_s^* \tag{A-2}$$

Substitution of Eq. (A-2) into Eq. (A-1) at $I_a = I_{La}$

$$I_{La} = \frac{FDX_o N_m}{\delta + \dfrac{DN_m}{k_2}} \tag{A-3}$$

Combination of Eqs. (A-1) and (A-3) along with the use of $I_{Lbd}(=Fk_2 X_o)$ to denote the limiting current imposed by the hydrogen transfer from the absorbed to the adsorbed state yields:

$$\begin{aligned} X_s &= X_o\left[1 - \left(\frac{1}{I_{La}} - \frac{1}{Fk_2 X_o}\right) I_a\right] \\ &= X_o\left[1 - \left(\frac{1}{I_{La}} - \frac{1}{I_{Lbd}}\right) I_a\right] \end{aligned} \tag{A-4}$$

Substitution of Eq. (A-4) into Eq. (12) and introduction of a new parameter, $K_t(=((K_2 - k_{-2})X_o)/((k_2 - k_{-2})X_o + k_{-2}))$, which is the interfacial hydrogen-transfer coefficient, results in the following equation:

$$\theta = \frac{\theta_o\left[1 - \dfrac{I_a}{I_{La}}\right]}{1 - K_t\left(\dfrac{1}{I_{La}} - \dfrac{1}{I_{Lbd}}\right) I_a} \tag{A-5}$$

Eq. (A-5) is the same as Eq. (16); X_o in Eq. (A-5) and $X_{\alpha\beta}$ in Eq. (16) both denote the initial concentration of hydrogen in the alloy.

Appendix B

B.1. Linearizing the current density for charge-transfer reaction

A function of two variables, $f(\theta,\eta)$, can be expanded about the point (θ_o,η_o) by the Taylor formula:

$$f(\theta,\eta) = f(\theta_o,\eta_o) + \sum_{j=1}^{\infty} \frac{1}{j}\left[\left(\delta\theta\frac{\partial}{\partial\theta} + \delta\eta\frac{\partial}{\partial\eta}\right)^j f(\theta,\eta)\right]_{(\theta_o,\eta_o)} \quad \text{(A-6)}$$

where $\delta\theta = \theta - \theta_o$, and $\delta\eta = \eta - \eta_o$. The expression in parentheses is a differential operator that is raised to the jth power. The various powers of $\partial/\partial\theta$, and $\partial/\partial\eta$ are symbols for repeated differentiation. After the operator acts on $f(\theta,\eta)$, the limits are taken for $f(\theta_o,\eta_o)$.

Consider the expansion of the current-overpotential Eq. (18):

$$f(\theta,\eta) = \frac{I_a}{I_o} = \frac{\theta}{\theta_o}\exp\left(\frac{\beta F}{RT}\eta\right) - \frac{1-\theta}{1-\theta_o}\exp\left[\frac{-(1-\beta)F}{RT}\eta\right] \quad \text{(A-7)}$$

The central point is chosen at $(\theta_o,0)$, where $I_a = 0$. If only the terms for $j = 1$ are kept, one obtains:

$$\frac{I_a}{I_o} = \left[\delta\theta\frac{\partial}{\partial\theta} + \delta\eta\frac{\partial}{\partial\eta}\right] f(\theta,\eta) \quad \text{(A-8)}$$

where the derivative is evaluated at $\theta_o,\eta = 0$.

Substituting for the derivatives and evaluating at the central point:

$$\frac{I_a}{I_o} = \frac{\theta-\theta_o}{\theta_o(1-\theta_o)} + \frac{F}{RT}\eta \quad \text{(A-9)}$$

which is equivalent to Eq. (47). By truncating the series at $j = 1$, a simple linear approximation has been derived from the more complex Eq. (18). It is valid for small excursions from the central point.

References

[1a] J.J.G. Willems, Philips J. Res. 39 (1984) .
[1b] J.J.G. Willems, K.H.J. Buschow, J. Less-Common Met. 129 (1987) 13.
[2] Q.M. Yang, M. Ciureanu, D.H. Ryan, O.J. Strom-Olsen, J. Electrochem. Soc. 141 (1994) 2108.
[3] P.H.L. Notten, P. Hokkeling, J. Electrochem. Soc. 138 (1991) 1877.
[4] C. Witham, A. Higtower, B. Fultz, B.V. Ratnakumar, R.C. Bowman Jr., J. Electrochem. Soc. 144 (1997) 3758.
[5] H.W. Yang, Y.Y. Wang, C.C. Wan, J. Electrochem. Soc. 143 (1996) 429.
[6] W. Zhang, M.P.S. Kumar, S. Srinivason, J. Electrochem. Soc. 142 (1995) 2935.
[7] G. Zheng, B.N. Popov, R.E. Whitem, J. Electrochem. Soc. 143 (1996) 435.
[8] G. Zheng, B.N. Popov, R.E. White, J. Appl. Electrochem. 28 (1998) 381.
[9] C.S. Wang, J. Electrochem. Soc. 145 (1998) 1801.
[10] B.V. Ratnakumar, C. Witham, R.C. Bowman Jr., A. Hightower, B. Fultz, J. Electrochem. Soc. 143 (1996) 2578.
[11] C.S. Wang, Y.Q. Lei, Q.D. Wang, Electrochim. Acta 43 (1998) 3193.
[12] B.E. Conway, J. Wojtowicz, J. Electroanal. Chem. 326 (1992) 277.
[13] S. Wakao, Y. Yonemura, J. Less-Common Met. 89 (1983) 481.
[14] H. Yayama, K. Kuroki, K. Hirvakawa, A. Tomokoyo, Jpn. J. Appl. Phys. 23 (1984) 1619.
[15] Q.M. Yang, M. Ciureanu, D.H. Ryan, J.O. Strom-Olsen, Electrochim. Acta 40 (1995) 1921.
[16] Q.M. Yang, M. Ciureanu, D. Ryan, J.O. Strom-Olsen, J. Electrochem. Soc. 141 (1994) 2113.